

Robust Variable Structure Controller Design for Fault Tolerant Flight Control

Dohyeon Kim and Youdan Kim
Seoul National University, Seoul 151-742, Republic of Korea

A model following control scheme is proposed that possesses fault detection and isolation capabilities as well as a fault tolerance property. The proposed model following controller is designed based on a variable structure control (VSC), and the scheme does not require the parameter estimation process for reconfigurable control. The main idea of the proposed algorithm stems from the fact that the nonlinear control of VSC counteracts external disturbances. The proposed algorithm is shown to be very useful for the case of control surface damage in aircraft, where the parameter change and external fault signal satisfy the matching conditions. The nonlinear control action that suppresses the fault effect can be used to determine how serious the damage is. Numerical results show the applicability of the proposed algorithm.

Nomenclature

A	= system matrix	K_m	= gain for output error feedback
A_m, B_m	= system/output matrix of the model to be followed	L_a	= stability derivative of roll moment with respect to a
a	= gain parameter for discontinuous control input	M	= basis of left annihilator of C_2
B	= input matrix	$m_{ail}, m_{rud}, m_{ele}$	= signals to be monitored to diagnose control surface damage
$b(t)$	= bounding function of $\ \xi_1(t)\ $	N_a	= stability derivative of roll moment with respect to a
C	= output matrix	$p(x, t)$	= $m \times n$ matrix i.e. $\Delta A = Bp$
C_1, C_2	= partitioned matrices of CT^T	r	= yaw rate
d_a	= ratio of lateral elevator location to aileron location from the body c.g.	S_a, S_r, S_v, S_w	= areas of aileron, rudder, vertical fin, wing
d_f	= fault effect vector, $px + hu + f$	s	= sliding variable
e	= state error, $x - x_m$	T	= transformation matrix
e_y	= output error, $y - y_m$	t_s	= time at which sliding motion starts
F	= sliding gain, for example, $(GC_2)^{-1}G$	u_d	= discontinuous control input
F_f	= feedforward gain to construct B_m i.e. $B_m = BF_f$	u_{eq}	= equivalent control
$f(t)$	= actuator fault vector	$u(t)$	= input vector
G	= sliding surface matrix	V_T	= total velocity of the aircraft
g	= acceleration of gravity	$x(t)$	= state vector
$h(x, u, t)$	= $m \times m$ matrix i.e. $\Delta B = Bh$	Y_a	= stability derivative of side force with respect to a
K	= state feedback gain to construct A_m i.e. $A_m = A - BK$	β	= sideslip angle
K_e	= gain for output error feedback	Γ	= $m \times n$ arbitrary matrix



Dohyeon Kim was born in Seoul, Korea, in 1970. He received his B.S., M.S., and Ph.D. degrees in aerospace engineering from Seoul National University in 1993, 1995, and 1998, respectively. Since 1999, he has been with the Department of Automotive Engineering at Woosuk University where he is now a faculty member. Prior to joining the university, he worked on a risk management system as a consultant at The Boston Consulting Group, Inc. His research interests include the application of modern control theory to the aerospace and ground vehicles, modeling and control of economic and mechanical systems, and fault tolerant control. He is a member of AIAA.



Youdan Kim is an Associate Professor in the Department of Aerospace Engineering of Seoul National University, Seoul, Korea. He also works for the Institute of Advanced Machinery and Design (IAMDD), Seoul National University. He received his B.S. and M.S. degrees in Aeronautical Engineering from Seoul National University, and Ph.D. degree in Aerospace Engineering from Texas A&M University, in 1983, 1985, and 1990, respectively. From 1990 to 1991, he worked as research associate at Texas A&M University, before he joined the faculty of the Seoul National University in 1992. His current research interests include the control system design for aircraft and spacecraft, trajectory optimization, and flexible structure control. He is a senior member of AIAA.

γ	= gain parameter for K_e
γ_e	= path angle of the aircraft at trim point
ΔA	= uncertainty/nonlinearity in system matrix
$\Delta A_{\text{ail}}, \Delta A_{\text{rud}}$	= ΔA caused by aileron/rudder damage
ΔB	= uncertainty/nonlinearity in input matrix
$\Delta B_{\text{ail}}, \Delta B_{\text{rud}}$	= ΔB caused by aileron/rudder damage
δ	= width of boundary layer
δ_a	= aileron deflection
δ_r	= rudder deflection
$\zeta_a, \zeta_r, \zeta_e$	= ratios of damaged area of aileron/rudder/elevator to their total areas
ζ'_a, ζ'_r	= ratios of damaged area of aileron/rudder to the overall wing area
θ_e	= pitch angle of the aircraft at trim point
$-\lambda_i$	= real part of i th eigenvalue of reduced-order matrix A_r
λ_{\min}	= $\min\{\lambda_i\}$
μ, σ	= conversion parameters of the moments of inertia
ρ	= bound for uncertainty and disturbance
ϕ	= roll angle

I. Introduction

FAULT tolerant control methodologies can be divided into two categories: passive fault tolerant systems and active fault tolerant control systems.¹ A control system that possesses enough robustness to cope with possible fault occurrence can be considered as a passive fault tolerant control system.^{2–5} An active fault tolerant control system, however, is defined as a control system that has the ability to accommodate fault by reconfiguring the control structure.

Active fault tolerant control procedures include the fault detection and isolation process and the control redesign (reconfiguration) process. The control redesign problem has been a challenging issue during the last decade.^{6–14} Previously proposed methods include the gain scheduling pseudoinverse method,^{7,8} feedback linearization,^{9–11} knowledge-based systems,¹ and the eigenstructure assignment technique.¹² A few recent works have utilized the linear model following method.^{13,14} However, the performances of the existing control reconfiguration methodologies depend on the accuracy of system identification that must be performed online.

In this study, we propose a fault tolerant model following control law based on the variable structure control (VSC) scheme. The proposed method does not require the control redesign process while it does possess the ability to detect and to isolate possible control surface damage.

An essential feature of VSC is nonlinear feedback control with discontinuity on the switching surfaces.^{15–17} The control is designed to drive the system to the predefined sliding surfaces and then to constrain the system state to remain there. The motion in the sliding surface, known as sliding motion, can be described as a low-order unforced system and is invariant to the parameter variation and external disturbances within the input channel. This inherent invariance enables fault tolerant performance in the face of control surface damage that satisfies the matching conditions without online (damaged) system identification. Recently, Shtessel and Tournes¹⁸ and Shtessel et al.¹⁹ designed a reconfigurable flight control system utilizing this invariance of VSC. The designed system achieves tracking performance after damage in the control surfaces without violating actuator limits.

The methodology proposed in this paper adopts the model following scheme, which minimizes bumps in the control reconfiguration stage, with VSC. Therefore, with the help of the invariance property, the method removes the toil of system identification, and, thus, the time required to cope with the faults is reduced. It is also clear that the parameters of VSC may be updated to improve the effectiveness of fault tolerant control when system identification is possible. In addition to utilizing the invariance property, the algorithm in this paper also makes use of the nonlinear control action to reconstruct the effects of control surface damage. This fault reconstruction concept has lately been introduced in VSC observer schemes,^{20,21} although they are much different from the algorithm in this paper. Because the methodology proposed in this paper is in the form of model following control, the sliding variables are computed from the out-

put errors, which reflects the effect of the control surface damage. Hence, the comparison of nonlinear control action and the adequate set of signals enable diagnosis of control surface damage.

The paper is constructed as follows. In Sec. II, a model following control scheme based on VSC is developed. The proposed control system satisfies the reaching condition and has the ability to reconstruct a certain set of faults. Section III describes modeling of the control surface damage. The result of a numerical simulation is given in Sec. IV to demonstrate the applicability of the proposed methodology.

II. VSC-Based Model Following Control

Problem Statement

Consider a system described by

$$\dot{\mathbf{x}}(t) = [A + \Delta A(x, t)]\mathbf{x}(t) + [B + \Delta B(x, t)]\mathbf{u}(t) + B\mathbf{f}(t) \quad (1)$$

$$\mathbf{y}(t) = C\mathbf{x}(t) \quad (2)$$

where $\mathbf{x}(t) \in R^n$ is a state vector, $\mathbf{u}(t) \in R^m$ is a control input vector, $\mathbf{y}(t) \in R^p$ is an output vector, and $\mathbf{f}(t) \in R^r$ ($r \leq m$) represents the possible added-form actuator fault with bounded magnitude. The matrices A , B , and C are real matrices with appropriate dimensions, and variations ΔA and ΔB denote uncertainty and nonlinearity in the plant and input parameters. We give the following assumptions.

Assumption 1: The pairs (A, B) and (A, C) are controllable and observable, respectively.

Assumption 2: There exist matrix functions $p(x, t)$ and $h(x, u, t)$ that satisfy the following matching conditions:

$$\Delta A(x, t) = Bp(x, t) \quad (3)$$

$$\Delta B(x, u, t) = Bh(x, u, t) \quad (4)$$

The physical meaning of this condition is that the variations and disturbances come through the input channel.

Assumption 3: The effects of uncertainty and disturbance are all bounded; there exists a known non-negative scalar ρ such that

$$\|px + hu + f\| \leq \rho \quad (5)$$

where $\|\cdot\|$ denotes an induced norm.

The reference model to be followed is described as

$$\dot{\mathbf{x}}_m(t) = A_m\mathbf{x}_m(t) + B_m\mathbf{r}(t) \quad (6)$$

$$\mathbf{y}_m(t) = C\mathbf{x}_m(t) \quad (7)$$

If the system described by Eqs. (1) and (2) follows the reference model selected as a nominal healthy closed-loop system, it can be said that the fault tolerant control objective is achieved. From this viewpoint, it is natural to choose the model system matrices as

$$A_m = A - BK \quad (8)$$

$$B_m = BF_f \quad (9)$$

where K is the state feedback gain chosen by considering system stability and performance, and F_f is the feedforward gain to track the command input.

Let us define the errors between the model and the plant state as

$$\mathbf{e}(t) = \mathbf{x}(t) - \mathbf{x}_m(t) \quad (10)$$

$$\mathbf{e}_y(t) = \mathbf{y}(t) - \mathbf{y}_m(t) = C\mathbf{e}(t) \quad (11)$$

Differentiating Eq. (10) with respect to time and substituting Eqs. (1), (2), (6), and (7) into the resulting equation yield

$$\begin{aligned} \dot{\mathbf{e}} &= (A + \Delta A)\mathbf{x} + (B + \Delta B)\mathbf{u} + B\mathbf{f} - A_m\mathbf{x}_m - B_m\mathbf{r} \\ &= A(\mathbf{x} - \mathbf{x}_m) + B\mathbf{u} + BK\mathbf{x}_m - B_m\mathbf{r} + B(px + hu + f) \\ &= A_m\mathbf{e} + B\mathbf{u} + BK\mathbf{x} - B_m\mathbf{r} + B(px + hu + f) \end{aligned} \quad (12)$$

Reaching Control

If it is possible to design a control law that makes the error dynamics described by Eq. (12) be stable even with the faults, then

the system described by Eq. (1) has a fault tolerant property. VSC is more useful for this purpose than any other reconfiguration strategy because it may assign desired characteristics to the transient error dynamics in addition to its inherent robustness. The space in which transient error lies is defined to be in the sliding mode, whose design is frequently called the sliding surface (or hyperplane) design. In this paper, a new sliding surface design scheme is proposed in the subsequent section.

Let us denote the sliding mode as

$$s(t) = Ge_y(t) = GC[x(t) - x_m(t)] = 0 \quad \forall t \geq t_s \quad (13)$$

where t_s is the time at which the sliding motion starts and the $m \times p$ matrix G is selected for GCB to be nonsingular. By the definition of the sliding mode, the velocity of $s(t)$ should also be zero,

$$\dot{s}(t) = G\dot{e}_y(t) = GC\dot{e}(t) = 0 \quad \forall t \geq t_s \quad (14)$$

By the use of Eqs. (12–14), the equivalent control can be obtained as

$$u_{eq} = -(GCB)^{-1}GC[A_me + BKx - B_mr + Bd_f] \quad (15)$$

where

$$d_f = px + hu + f \quad (16)$$

Substituting u_{eq} into Eq. (12) yields

$$\begin{aligned} \dot{e} &= [I - B(GCB)^{-1}GC][A_me + BKx - B_mr + Bd_f] \\ &= [I - B(GCB)^{-1}GC]A_me \end{aligned} \quad (17)$$

Therefore, gain matrix G should be selected in consideration of the eigenvalues of the $[I - B(GCB)^{-1}GC]A_m$ matrix. The procedure for designing sliding surface G will be summarized in the next section.

To reach the designed sliding mode, a number of control strategies can be used: relays with either fixed- or state-dependent gains, linear feedback with switched gains, and widely used unit-vector-type controls. In this paper, a simple control structure is proposed as follows.

Lemma: A control in the form of

$$u(t) = -Kx_m + K_e e_y + K_m r + u_d \quad (18)$$

where

$$K_e = -\gamma(GCB)^{-1}G, \quad K_m = (GCB)^{-1}GCB_m = F_f$$

$$u_d = a(GCB)^{-1}\|GCB\|\text{sgn}(s), \quad \text{sgn}(s) = \text{sgn} \left\{ \begin{bmatrix} s_1 \\ s_2 \\ \vdots \\ s_m \end{bmatrix} \right\}$$

and a and γ are scalar parameters, satisfies the reaching condition of

$$\frac{d}{dt} \left[\frac{1}{2}(s^T s) \right] < 0 \quad (19)$$

under Assumptions 1–3

Proof: Using Eqs. (12–14), we obtain

$$\begin{aligned} s^T \dot{s} &= s^T G\dot{e}_y \\ &= s^T GC[A_me + Bu + BKx - B_mr + Bd_f] \\ &= s^T GC[Ae + BK_e Ce + Bd_f + Bu_d] \\ &= s^T \{GC[A - \gamma B(GCB)^{-1}GC]e + GC(Bd_f + Bu_d)\} \\ &= s^T \{GC(A - \gamma I)e + GCB(d_f + u_d)\} \\ &= e^T C^T G^T GC(A - \gamma I)e + s^T GCB(d_f + u_d) \end{aligned} \quad (20)$$

If $(A - \gamma I)$ is negative definite, Eq. (20) becomes

$$\begin{aligned} s^T \dot{s} &= -e^T C^T G^T GC Q^T Qe + s^T GCBd_f + as^T \|GCB\|\text{sgn}(s) \\ &\leq \|s\| \|GCB\| \|d_f\| + a\|GCB\|s^T \text{sgn}(s) \end{aligned} \quad (21)$$

By consideration of the Assumptions, the preceding inequality can be written as

$$s^T \dot{s} \leq \|GCB\|[\rho\|s\| + as^T \text{sgn}(s)] \quad (22)$$

Hence, the reaching condition is achieved by selecting a sufficiently large value of a , that is, $a < -\rho$. \square

During the sliding motion, the high-frequency chattering of discontinuous control can be present around the switching surface. This chattering behavior of the actuator could result in continuous saturation or excitation of high-order dynamics. This continuous saturation is especially hazardous in aerospace applications because it may cause pilot-induced oscillations.²² To overcome this chattering problem, several methods replacing the discontinuous control with a nonlinear continuous one have been suggested. In this paper, a simple saturating control is adopted as

$$\text{sat}(s/\delta) = \begin{cases} 1 & \text{if } s > \delta \\ s/\delta & \text{if } |s| < \delta \\ -1 & \text{if } s < -\delta \end{cases} \quad (23)$$

where the positive scalar δ is a design parameter that depends on the system. Within the boundary layer or $-\delta < s < \delta$, control is linear, whereas it is identical to the original relay outside the boundary layer. With this control, the system is driven to the boundary layer (near the sliding motion), not to the exact sliding surface $s = 0$. As a result, chattering is removed; however, invariance is degraded at the same time.

Sliding Surface Design

Design of sliding surfaces is equivalent to prescribing a reduced-order dynamics of the system on the sliding surface, which is the transient dynamics of error. The design techniques for state feedback are mainly due to Refs. 23 and 24. Sliding surface design techniques for output feedback VSC are under development.^{25–27} In this paper, a simple algorithm modified from Ref. 25 is used. Let us start with the dynamics extracted from Eq. (12). Note that the other terms in Eq. (12) have no effect after reaching sliding motion, which can be seen in Eq. (17):

$$\dot{e} = A_me + Bu \quad (24)$$

$$e_y = Ce \quad (25)$$

Consider an orthogonal transformation by setting $z = Te$, where the transformation matrix T is defined so that

$$TB = \begin{bmatrix} 0 \\ B_2 \end{bmatrix} \quad (26)$$

Partitioning z as $[z_1^T \ z_2^T]^T$, where $z_1 \in R^{n-m}$ and $z_1 \in R^m$, yields

$$\dot{z}_1 = A_{11}z_1 + A_{12}z_2, \quad \dot{z}_2 = A_{21}z_1 + A_{22}z_2 + B_2u \quad (27)$$

$$e_y = [C_1 \ C_2]z \quad (28)$$

where

$$\begin{bmatrix} A_{11} & A_{12} \\ A_{21} & A_{22} \end{bmatrix} = T A_m T^T, \quad [C_1 \ C_2] = C T^T$$

The sliding dynamics can be written as

$$s = 0 = GCe = GC_1 z_1 + GC_2 z_2 \quad (29)$$

Therefore, Eqs. (27) and (28) can be written as

$$\dot{z}_1 = (A_{11} - A_{12}FC_1)z_1 \quad (30)$$

$$e_y = (I_p - C_2F)C_1 z_1 \quad (31)$$

where

$$F = (GC_2)^{-1}G \quad (32)$$

As we can see, the sliding surface design is to assign the eigenvalues of $(A_{11} - A_{12}FC_1)$ to the desired values under the constraint of $FC_2 = I_m$.

The solution of Eq. (32) can be obtained as

$$F = C_2^{-L} + \Gamma M^T \quad (33)$$

where C_2^{-L} is the left inverse of C_2 , M is the basis of the left annihilator of C_2 , that is, $M^T C_2 = 0$, and Γ is an $m \times p$ arbitrary matrix.

The design procedure can be summarized as follows.

1) Find Γ such that $(\hat{A}_{11} - A_{12}\Gamma\hat{C}_1)$ has the desired spectrum, where

$$\hat{A}_{11} = A_{11} - A_{12}C_2^{-L}, \quad \hat{C}_1 = M^T C_1$$

2) Compute F using Eq. (33).

3) Find G using the relation $G(I_m - C_2F) = 0$.

Fault Reconstruction

The control of Eq. (18) with Eq. (23) yields the error equation:

$$\dot{e} = [A - \gamma B(GCB)^{-1}GC]e + B(d_f + u_d) \quad (34)$$

The transformation of $\xi = Te$ with matrix T defined in Eq. (26) yields

$$\dot{\xi} = T[A - \gamma B(GCB)^{-1}GC]T^T\xi + TB(u_d + d_f) \quad (35)$$

By partitioning $\xi = [\xi_1 \ \xi_2]^T$, Eq. (35) can be written as

$$\dot{\xi}_1 = A_{11}\xi_1 + A_{12}\xi_2, \quad \dot{\xi}_2 = A_{21}^s\xi_1 + A_{22}^s\xi_2 + B_2(u_d + d_f) \quad (36)$$

where

$$\begin{bmatrix} A_{21}^s & A_{22}^s \end{bmatrix} = [A_{21} \ A_{22}] + B_2[K - \gamma(GCB)^{-1}GC]T^T \quad (37)$$

The sliding variable and its derivative can be written as

$$s = GC_1\xi_1 + GC_2\xi_2 \quad (38)$$

$$\dot{s} = GC_1\dot{\xi}_1 + GC_2\dot{\xi}_2 \quad (39)$$

Equation (38) can be rewritten as

$$\xi_2 = (GC_2)^{-1}(-GC_1\xi_1 + s) \quad (40)$$

and Eq. (30) becomes

$$\begin{aligned} \dot{s} &= GC_1\dot{\xi}_1 + GC_2\dot{\xi}_2 \\ &= [GC_1(A_{11} - A_{12}FC_1) + GC_2(A_{21}^s - A_{22}^sFC_1)]\xi_1 \\ &\quad + (GC_1A_{12} + GC_2A_{22}^s)(GC_2)^{-1}s + GC_2B_2(u_d + d_f) \\ &= [GC_1(A_{11} - A_{12}FC_1) - GC_2(A_{21}^s - A_{22}^sFC_1)]\xi_1 \\ &\quad + \{(a/\delta)\|GC_2B_2\|I + (GC_1A_{12} + GC_2A_{22}^s)(GC_2)^{-1}\}s \\ &\quad + GC_2B_2d_f \end{aligned} \quad (41)$$

Equation (41) governs the dynamics of sliding variable s in the boundary layer and can be simplified as

$$\dot{s} = Ls + M\xi_1 + Nd_f \quad (42)$$

where

$$\begin{aligned} L &= (a/\delta)\|GC_2B_2\|I + (GC_1A_{12} + GC_2A_{22}^s)(GC_2)^{-1} \\ M &= [GC_1(A_{11} - A_{12}FC_1) - GC_2(A_{21}^s - A_{22}^sFC_1)] \\ N &= GC_2B_2 \end{aligned} \quad (43)$$

We propose the following simple theorem modified from Ref. 26.

Theorem: Let $(A_{11} - A_{12}FC_1)$ be A_r and the real parts of the $n-m$ eigenvalues be $\{-\lambda_1, -\lambda_2, \dots, -\lambda_{n-m}\}$. Here λ_{\min} is defined as the minimum value of $\{\lambda_1, \lambda_2, \dots, \lambda_{n-m}\}$. Then, we have the following:

1) For some real γ , $\|e^{A_r t}\| < \gamma e^{-\lambda_{\min} t}$.

2) Here $\|\xi_1(t)\|$ is bounded by $b(t)$ after a finite period of time, where $b(t)$ is the solution of the following equation:

$$\dot{b}(t) = -\lambda_b b(t) + \gamma \delta \|A_{12}(GC_2)^{-1}\| \quad (44)$$

where $\lambda_b < \lambda_{\min}$ and $b(0) > 0$.

Proof: Because part 1 is obvious, consider part 2. The insertion of Eq. (40) into Eq. (36) yields

$$\dot{\xi}_1 = A_r \xi_1 + A_{12}(GC_2)^{-1}s \quad (45)$$

which has the solution of

$$\xi_1(t) = e^{A_r t} \xi_1(0) + \int_0^t e^{A_r(t-\tau)} A_{12}(GC_2)^{-1}s \, d\tau \quad (46)$$

Therefore,

$$\|\xi_1(t)\| \leq \gamma e^{-\lambda_{\min} t} \|\xi_1(0)\| + \int_0^t \gamma e^{-\lambda_{\min}(t-\tau)} \|A_{12}(GC_2)^{-1}\| \|s\| \, d\tau \quad (47)$$

Because $\|s\| \leq \delta$ in the boundary layer, Eq. (47) can be written as

$$\|\xi_1(t)\| \leq \gamma e^{-\lambda_{\min} t} \|\xi_1(0)\| + \gamma \delta \int_0^t \gamma e^{-\lambda_{\min}(t-\tau)} \|A_{12}(GC_2)^{-1}\| \, d\tau \quad (48)$$

The solution of Eq. (44) is

$$b(t) = e^{-\lambda_b t} b(0) + \gamma \delta \int_0^t e^{-\lambda_{\min}(t-\tau)} \|A_{12}(GC_2)^{-1}\| \, d\tau \quad (49)$$

Therefore, comparison of Eqs. (48) and (49) shows $\|\xi_1(t)\| \leq b(t)$ after a finite period of time, with $b(0) > 0$ and $\lambda_b < \lambda_{\min}$. \square

Consider Eq. (42) again. If fault or parameter variation represented by d_f occurs at a certain time, the perturbed sliding variable moves toward the sliding surface. After that, the dynamics of the sliding variable is governed by Eq. (42) inside the boundary layer. After a sufficient time period, ξ_1 in Eq. (42) has a small value whose norm is bounded by $(\gamma \delta / \lambda_m) \|A_{12}(GC_2)^{-1}\|$. Because the values δ and γ are naturally very small and λ_m can be made to be large, the effect of ξ_1 might be negligible thereafter.

Therefore, we can approximate Eq. (42) as

$$\dot{s} \approx Ls + Nd_f \quad (50)$$

The steady-state value of the sliding variable is then

$$s_{ss} \approx -L^{-1}Nd_{fss} \quad (51)$$

or

$$d_f \approx -N^{-1}Ls \quad (52)$$

Hence, monitoring the sliding variable enables the reconstruction of the fault that can be characterized by Eq. (16) and Assumption 2.

III. Control Surface Damage Model

The linear equation of aircraft lateral motion is

$$\begin{bmatrix} \dot{\beta} \\ \dot{\phi} \\ \dot{p} \\ \dot{r} \end{bmatrix} = \begin{bmatrix} \frac{Y_\beta}{V_T} & \frac{g \cos \theta_e}{V_T} & \frac{Y_p}{V_T} & \frac{Y_r}{V_T} \\ 0 & 0 & \frac{\cos \gamma_e}{\cos \theta_e} & \frac{\sin \gamma_e}{\cos \theta_e} \\ \mu L_\beta + \sigma_1 N_\beta & 0 & \mu L_p + \sigma_1 N_p & \mu L_r + \sigma_1 N_r \\ \mu N_\beta + \sigma_2 L_\beta & 0 & \mu N_p + \sigma_2 L_p & \mu N_r + \sigma_2 L_r \end{bmatrix} \begin{bmatrix} \beta \\ \phi \\ p \\ r \end{bmatrix} + \begin{bmatrix} \frac{Y_{\delta_a}}{V_T} & \frac{Y_{\delta_r}}{V_T} \\ 0 & 0 \\ \mu L_{\delta_a} + \sigma_1 N_{\delta_a} & \mu L_{\delta_r} + \sigma_1 N_{\delta_r} \\ \mu N_{\delta_a} + \sigma_2 L_{\delta_a} & \mu N_{\delta_r} + \sigma_2 L_{\delta_r} \end{bmatrix} \begin{bmatrix} \delta_a \\ \delta_r \end{bmatrix} \quad (53)$$

where the state vector consists of the sideslip angle β , the roll angle ϕ , the roll rate p , and the yaw rate r . Inputs are the aileron deflection

δ_a and the rudder deflection δ_r . All of the notations used for the elements are in standard fashion, in accordance with Ref. 28. The stability derivatives Y_a , L_a , and N_a are defined in the traditional manner; the subscript e attached to the path angle and the pitch angle denotes trim values. The coefficients μ and σ_i are related to the conversion of the moment of inertia from the body axis to the stability axis,

$$\mu = \frac{J'_z J'_x}{J_x J_z - J_{xz}} \quad (54)$$

$$\sigma_1 = \frac{J'_x J'_{xz}}{J_x J_z - J_{xz}} \quad (55)$$

$$\sigma_2 = \frac{J'_x J'_{xz}}{J_x J_z - J_{xz}} \quad (56)$$

In the preceding equations, the moments of inertia in the numerator are measured in the stability axis of the system, whereas those in numerator are measured in body axis.²⁸

Consider the parameter variations for the case in which some parts of a control surface are damaged. The changes of system and input matrices can be modeled by analyzing the stability and control derivatives. References 29 and 30 deal with this interesting topic.

If the aileron is damaged, the changes of system matrices can be formulated as

$$\Delta A_{\text{ail}} = B p_{\text{ail}} \approx B \left\{ (\zeta'_a - 1) \begin{bmatrix} \mu L_{\delta_a} + \sigma_1 N_{\delta_a} & \mu L_{\delta_r} + \sigma_1 N_{\delta_r} \\ \mu N_{\delta_a} + \sigma_2 L_{\delta_a} & \mu N_{\delta_r} + \sigma_2 L_{\delta_r} \end{bmatrix}^{-1} \begin{bmatrix} \mu L_\beta & 0 & \mu L_p & 0 \\ 0 & 0 & 0 & 0 \end{bmatrix} \right\} \approx B \left\{ (\zeta'_a - 1) \begin{bmatrix} L_{\delta_a} & L_{\delta_r} \\ N_{\delta_a} & N_{\delta_r} \end{bmatrix}^{-1} \begin{bmatrix} L_\beta & 0 & L_p & 0 \\ 0 & 0 & 0 & 0 \end{bmatrix} \right\} \quad (62)$$

$$\Delta B_{\text{ail}} = B h_{\text{ail}} = B \left\{ (\zeta'_a - 1) \begin{bmatrix} 1 & 0 \\ 0 & 0 \end{bmatrix} \right\} \quad (63)$$

$$\begin{aligned} \Delta A_{\text{rud}} = B p_{\text{rud}} &\approx B \left\{ (\zeta'_r - 1) \begin{bmatrix} \mu L_{\delta_a} + \sigma_1 N_{\delta_a} & \mu L_{\delta_r} + \sigma_1 N_{\delta_r} \\ \mu N_{\delta_a} + \sigma_2 L_{\delta_a} & \mu N_{\delta_r} + \sigma_2 L_{\delta_r} \end{bmatrix}^{-1} \begin{bmatrix} \mu L_\beta + \sigma_1 N_\beta & 0 & \mu L_p + \sigma_1 N_p & \mu L_r + \sigma_1 N_r \\ \mu N_\beta + \sigma_2 L_\beta & 0 & \mu N_p + \sigma_2 L_p & \mu N_r + \sigma_2 L_r \end{bmatrix} \right\} \\ &\approx B \left\{ (\zeta'_r - 1) \begin{bmatrix} L_{\delta_a} & L_{\delta_r} \\ N_{\delta_a} & N_{\delta_r} \end{bmatrix}^{-1} \begin{bmatrix} L_\beta & 0 & L_p & L_r \\ N_\beta & 0 & N_p & N_r \end{bmatrix} \right\} \end{aligned} \quad (64)$$

$$\Delta A = \Delta A_{\text{ail}} = (\zeta'_a - 1) \begin{bmatrix} 0 & 0 & 0 & 0 \\ 0 & 0 & 0 & 0 \\ \mu L_\beta & 0 & \mu L_p & 0 \\ 0 & 0 & 0 & 0 \end{bmatrix} \quad (57)$$

$$\Delta B = \Delta B_{\text{ail}} = (\zeta'_a - 1) \begin{bmatrix} Y_{\delta_a}/V_T & 0 \\ 0 & 0 \\ \mu L_{\delta_a} + \sigma_1 N_{\delta_a} & 0 \\ \mu N_{\delta_a} + \sigma_2 L_{\delta_a} & 0 \end{bmatrix} \quad (58)$$

where the factor ζ'_a is the ratio of the damaged area to the total aileron area and ζ'_a is the ratio of the damaged area to the overall wing.²⁹

Similarly, the rudder damage can be described by the following matrix with ζ'_r and ζ'_r :

$$\begin{aligned} \Delta A = \Delta A_{\text{rud}} &= (\zeta'_r - 1) \\ &\times \begin{bmatrix} Y_\beta/V_T & 0 & Y_p/V_T & Y_r/V_T \\ 0 & 0 & 0 & 0 \\ \mu L_\beta + \sigma_1 N_\beta & 0 & \mu L_p + \sigma_1 N_p & \mu L_r + \sigma_1 N_r \\ \mu N_\beta + \sigma_2 L_\beta & 0 & \mu N_p + \sigma_2 L_p & \mu N_r + \sigma_2 L_r \end{bmatrix} \end{aligned} \quad (59)$$

$$\Delta B = \Delta B_{\text{rud}} = (\zeta'_r - 1) \begin{bmatrix} 0 & Y_{\delta_r}/V_T \\ 0 & 0 \\ 0 & \mu L_{\delta_r} + \sigma_1 N_{\delta_r} \\ 0 & \mu N_{\delta_r} + \sigma_2 L_{\delta_r} \end{bmatrix} \quad (60)$$

The assumption that the longitudinal and lateral motions are decoupled is no longer valid if the elevator is damaged. Once an elevator on one side operates with less surface area, it produces less moment than the other elevator about the roll axis of the aircraft. This moment can be modeled as a disturbance term added to Eq. (53):

$$B f_{\text{elev}} = d_a (1 - \zeta_e) \begin{bmatrix} 0 \\ 0 \\ \mu L_{\delta_a} + \sigma_1 N_{\delta_a} \\ \mu N_{\delta_a} + \sigma_2 L_{\delta_a} \end{bmatrix} \delta_e \quad (61)$$

where d_a is the ratio of the lateral elevator location to the aileron location from the body center of mass, ζ_e is the ratio of the damaged elevator area to the total elevator area, and δ_e is the elevator deflection.

Note from Eqs. (57–61) that the parameters' change due to the control surface damages do not satisfy Assumption 2. However, for conventional aircraft, those variations approximately satisfy the matching conditions. This is because the values of μ are much larger than those of σ_i for most aircraft.

$$\Delta B_{\text{rud}} = B h_{\text{rud}} = B \left\{ (\zeta'_r - 1) \begin{bmatrix} 0 & 1 \\ 0 & 1 \end{bmatrix} \right\} \quad (65)$$

Therefore, the FDI and fault tolerant control algorithm developed in Sec. II can now be applied to the control surface damage problem. The \mathbf{d}_f are

$$\begin{aligned} (\mathbf{d}_f)_{\text{ail}} &= p_{\text{ail}} \mathbf{x} + h_{\text{ail}} \mathbf{u} \triangleq (\zeta'_a - 1) p_{\text{Eail}} \mathbf{x} + (\zeta'_a - 1) h_{\text{Eail}} \mathbf{u} \\ &= (\zeta'_a - 1) \{ [S_a / (S_v + S_w)] p_{\text{Eail}} \mathbf{x} + h_{\text{Eail}} \mathbf{u} \} \end{aligned} \quad (66)$$

$$\begin{aligned} (\mathbf{d}_f)_{\text{rud}} &= p_{\text{rud}} \mathbf{x} + h_{\text{rud}} \mathbf{u} \triangleq (\zeta'_r - 1) p_{\text{Erud}} \mathbf{x} + (\zeta'_r - 1) h_{\text{Erud}} \mathbf{u} \\ &= (\zeta'_r - 1) \{ (S_r / S_v) p_{\text{Erud}} \mathbf{x} + h_{\text{Erud}} \mathbf{u} \} \end{aligned} \quad (67)$$

$$(\mathbf{d}_f)_{\text{elev}} = f'_{\text{elev}} = d_a (1 - \zeta_e) \begin{bmatrix} \delta_e \\ 0 \end{bmatrix} \quad (68)$$

where S_a , S_v , S_w , and S_r denote areas of aileron, vertical fin, wing, and rudder, respectively.

Let us define the signals as

$$m_{\text{ail}} \triangleq \{ [S_a / (S_v + S_w)] p_{\text{Eail}} \mathbf{x} + h_{\text{Eail}} \mathbf{u} \} \quad (69)$$

$$m_{\text{rud}} \triangleq \{ (S_r / S_v) p_{\text{Erud}} \mathbf{x} + h_{\text{Erud}} \mathbf{u} \} \quad (70)$$

$$m_{\text{ele}} \triangleq d_a \begin{bmatrix} \delta_e \\ 0 \end{bmatrix} \quad (71)$$

Therefore, if the signals m_{ail} , m_{rud} , and m_{ele} were to be monitored in flight and compared to the shape of the signal produced by Eq. (52), then the kind of damage could be detected whereas the quantity of damage could be diagnosed by way of the ratio of the signal being monitored and the computed signal $d_f \approx -N^{-1}Ls$.

IV. Numerical Simulation and Verification

Consider an F-16 aircraft in steady-state pull-up motion.²⁸ The system can be written as

$$\begin{bmatrix} \dot{\beta} \\ \dot{\phi} \\ \dot{p} \\ \dot{r} \end{bmatrix} = \begin{bmatrix} -0.322 & 0.0612 & 0.298 & -0.948 \\ 0 & 0.0930 & 1 & 0.310 \\ -62.5 & 0 & -3 & 1.99 \\ 7.67 & 0 & -0.262 & -0.629 \end{bmatrix} \begin{bmatrix} \beta \\ \phi \\ p \\ r \end{bmatrix} + \begin{bmatrix} 0.0003 & 0.00002 \\ 0 & 0 \\ -0.645 & 0.126 \\ -0.0180 & -0.6667 \end{bmatrix} \begin{bmatrix} \delta_a \\ \delta_r \end{bmatrix}$$

Because the model is acquired by the numerical linearization of a nonlinear model, the (2,2) element has a nonzero element that is not expected in algebraic linearization. The measured outputs are selected to be the sideslip angle and two angular rates.

The reference model is constructed by using the linear quadratic method, which yields

$$K = \begin{bmatrix} 5.28 & -1.2631 & -0.8921 & -0.5381 \\ 18.0291 & -2.9473 & -0.1677 & -7.3834 \end{bmatrix}$$

$$F_f = \begin{bmatrix} -84.2926 & 12.7196 & 21.6319 \\ 26.7187 & 25.7248 & -16.2008 \end{bmatrix}$$

The sliding surface that is designed according to the procedure in Sec. II is

$$G = \begin{bmatrix} 0 & -0.2463 & 0.9692 \\ -0.9999 & -0.0116 & 10.4117 \end{bmatrix}$$

Thus, the dynamics in the sliding motion, or transient error dynamics, is governed by the eigenvalues as

$$\lambda(A_{11} - A_{12}FC_1) = \begin{bmatrix} -3.5645 \\ -1.4359 \end{bmatrix}$$

With these results, the reaching control law proposed by the Lemma can be designed. In this particular numerical example, the parameters are set to be $\gamma = 10$ and $a = -1$. For the saturating control as in Eq. (23), $\delta = 0.001$ is used for each sliding variable.

Let us first consider the rudder damage case. Assume that the damage occurs at 2 s with the value of $\zeta_r = 0.8$, which corresponds to a 20% loss of the rudder surface. Figure 1 shows the performance of the fault tolerant model following control system. The reference input to the model is a step sideslip angle with a magnitude of 0.1 rad. In spite of the damage occurring at 2 s, the outputs of the plant follow the reference model well after a short transient period. The control input to the plant can be seen in Fig. 2. The nonlinear control component is activated at 2 s to make up for the rudder loss.

Figures 3 and 4 verify the FDI capability of the proposed algorithm. The shape of the signal m_{rud} has the same shape of $d_f \approx -N^{-1}Ls$ after a short transient period. Therefore, the detection can be achieved, and as predicted in Eq. (67), the ratio of the two signals is $(\zeta_r - 1)$.

Consider the elevator damage case. The elevator deflection is assumed to be a sine wave, and it acts as a disturbance, as seen in Eq. (61). The model following performance shown in Fig. 5 verifies the robustness of the proposed algorithm. The coupling effect of

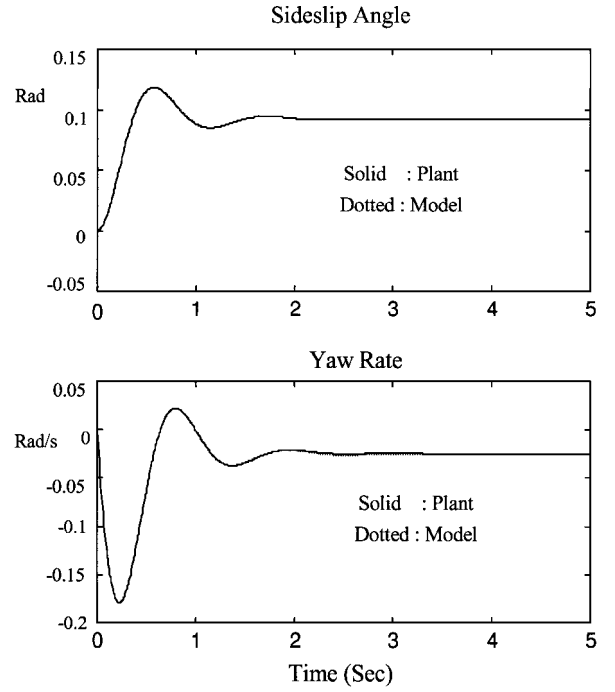


Fig. 1 Model following performance (rudder damage case).

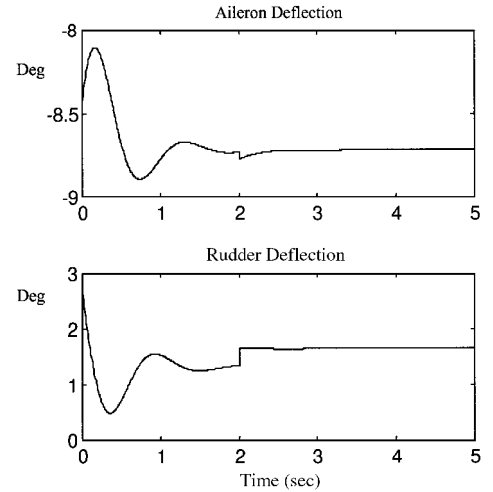


Fig. 2 Control input history (rudder damage case).

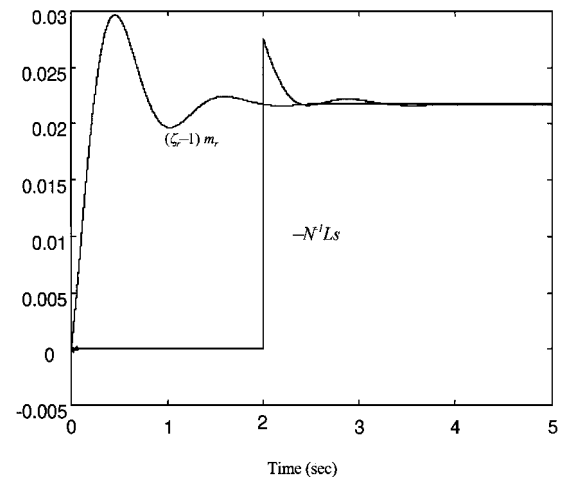


Fig. 3 Monitored signal and computed fault effect, first element (rudder damage case).

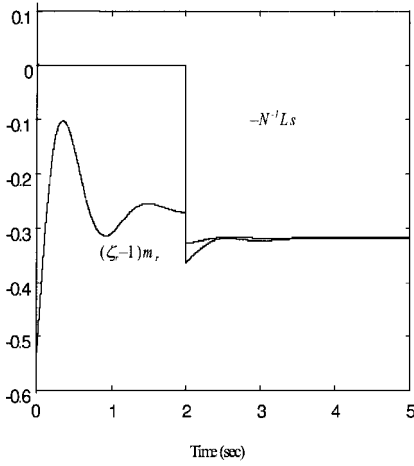


Fig. 4 Monitored signal and computed fault effect, second element (rudder damage case).

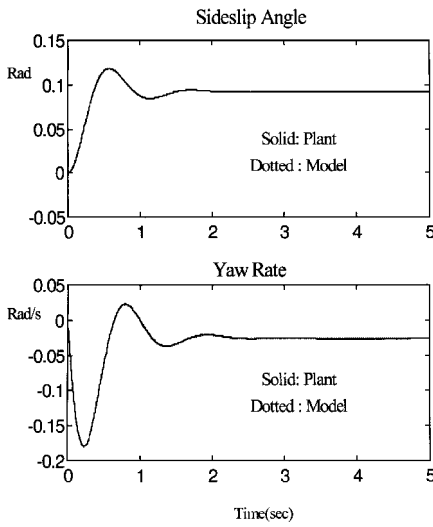


Fig. 5 Model following performance (elevator damage case).

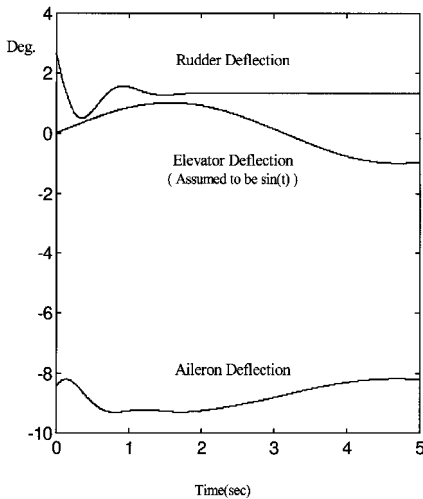


Fig. 6 Control input history and assumed elevator deflection (elevator damage case).

the elevator damage is well damped by the nonlinear control as seen in Fig. 6. Figure 7 shows the relation between the monitored signal $d_a[\delta_e 0]^T$ and the computed signal $d_f \approx -N^{-1}Ls$. It can be concluded that fault diagnosis is possible because the monitored signal multiplied by $1 - \zeta_e = 0.2$ is almost the same as the computed signal, even though the matching condition is not exactly satisfied in this case. The small errors between the two signals come from this discrepancy.

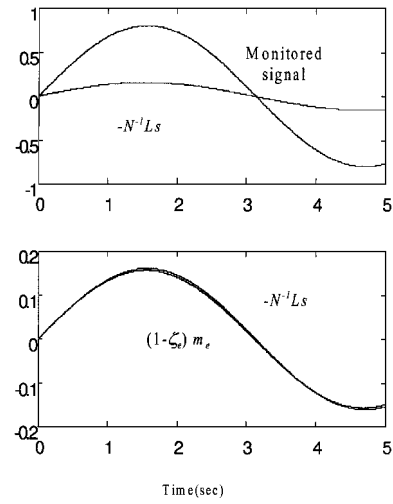


Fig. 7 Monitored signal and computed fault effect (elevator damage case).

V. Conclusions

The model following control scheme based on VSC developed in this paper satisfies the reaching condition and has the ability to reconstruct a certain set of faults. With the help of the invariance property, the work of system identification can be avoided, and, thus, the time required to cope with the faults is reduced. The proposed algorithm can also reconstruct the effects of control surface damage by analyzing nonlinear control action. The comparison of nonlinear control action and the adequate set of signals enable diagnosis of control surface damage. The proposed algorithm would be a useful alternative to the existing fault tolerant control schemes that mostly require a precise parameter estimation process. The applicability of the algorithm proposed has been shown with the F-16 aircraft with control surface damages. While maintaining satisfactory model following performance, the algorithm successfully diagnosed the damages that occurred in the aircraft.

References

- Handelmann, D. A., and Stengel, R. F., "Combining Expert System and Analytical Redundancy Concepts for Fault Tolerance Flight Control," *Journal of Guidance, Control, and Dynamics*, Vol. 12, No. 1, 1989, pp. 39-45.
- Etemo, J. S., Looze, D. P., and Willsky, A. S., "Design Issues for Fault-Tolerant Restructurable Aircraft Control," *Proceedings of 24th IEEE Conference on Decision and Control*, Inst. of Electrical and Electronics Engineers, New York, 1985, pp. 900-905.
- Stengel, R. F., "Toward Intelligent Flight Control," *IEEE Transactions on Systems, Man, and Cybernetics*, Vol. 23, No. 6, 1996, pp. 1699-1716.
- Tyler, M., and Morari, M., "Optimal and Robust Design of Integrated Control and Diagnostic Modules," *Proceedings of American Control Conference '94*, Baltimore, MD, 1994, pp. 2060-2064.
- Stroupstrup, J., and Grimbale, M. J., "Integrating Control and Fault Diagnosis: A Separation Result," *Proceedings of IFAC Symposium on Fault Detection, Supervision and Safety for Technical Processes--SAFEPROCESS 97*, IFAC, Hull, UK, 1997, pp. 323-328.
- Patton, R. J., "Fault Tolerant Control: the 1997 Situation (Survey)," *Proceedings of IFAC SAFEPROCESS '97*, IFAC, Hull, UK, 1997, pp. 1033-1055.
- Rattan, K. S., "Evaluation of Control Mixer Concept for Reconfiguration of Flight Control Systems," *Proceedings of National Aerospace and Electronics Conference*, Inst. of Electrical and Electronics Engineers, New York, 1985, pp. 560-569.
- Gao, Z., and Antsaklis, P. J., "Stability of the Pseudo-inverse Method for Reconfigurable Control Systems," *International Journal of Control*, Vol. 53, No. 3, 1991, pp. 717-729.
- Smith, G. A., and Meyer, G., "Aircraft Automatic Flight Control System with Model Inversion," *Journal of Guidance, Control, and Dynamics*, Vol. 10, No. 3, 1987, pp. 269-275.
- Lane, S. H., and Stengel, R. F., "Flight Control Design Using Non-Linear Inverse Dynamics," *Automatica*, Vol. 24, No. 4, 1988, pp. 471-483.
- Ochi, Y., and Kanai, K., "Design of Restructurable Flight Control Systems Using Feedback Linearisation," *Journal of Guidance, Control, and Dynamics*, Vol. 14, No. 5, 1991, pp. 903-911.
- Jiang, J., "Design of Reconfigurable Control Systems Using Eigenstructure Assignments," *International Journal of Control*, Vol. 59, No. 2, 1994, pp. 395-410.

¹³Caglayan, A. K., Rahnamai, K., and Alien, S. M., "Detection, Identification and Estimation of Surface Damage/Actuator Failure for High Performance Aircraft," *Proceedings of American Control Conference '88*, American Automatic Control Council, Greenvalley, AZ, 1988, pp. 2206–2212.

¹⁴Dhayagude, N., and Gao, Z., "A Novel Approach to Reconfigurable Control System Design," *Journal of Guidance, Control, and Dynamics*, Vol. 19, No. 4, 1996, pp. 963–967.

¹⁵Hung, J. Y., Gao, W., and Hung, J. C., "Variable Structure Control: A Survey," *IEEE Transactions on Industrial Electronics*, Vol. 40, No. 1, 1993, pp. 2–21.

¹⁶DeCarlo, R. A., Zak, S. H., and Matthews, G. P., "Variable Structure Control of Nonlinear Multivariable Systems: A Tutorial," *Proceedings of the IEEE*, Vol. 76, No. 3, 1988, pp. 212–233.

¹⁷Zinober, A. S. I. (ed.), *Deterministic Control of Uncertain Systems*, Inst. of Electrical Engineers, Control Engineering Series, Peter Peregrinus London, 1990.

¹⁸Shtessel, Y. B., and Tournes, C. H., "Flight Control Reconfiguration on Sliding Modes," *Proceedings of AIAA Guidance, Control, and Control Conference*, AIAA, Reston, VA, 1997, pp. 1288–1298.

¹⁹Shtessel, Y. B., Buffington, J., Pachter, M., Chandler, P., and Banda, S., "Reconfigurable Flight Control on Sliding Modes Addressing Actuator Deflection and Deflection Rate Saturation," *Proceedings of AIAA Guidance, Control, and Control Conference*, AIAA, Reston, VA, 1998, pp. 127–137.

²⁰Hermans, F. J. J., and Zarrop, M. B., "Sliding Mode Observers for Robust Sensor Monitoring," Univ. of Science and Technology in Manchester, Control System Center, Rept. 830, Manchester, June 1995.

²¹Edwards, C., Spurgeon, S. K., Patton, R. J., and Klozek, P., "Sliding Mode Observers for Fault Detection," *Proceedings of IFAC SAFEPROCESS '97*, IFAC, Hull, UK, 1997, pp. 522–527.

²²Thurkral, A., and Innocenti, M., "Control Design Challenge: A Variable Structure Approach," *Journal of Guidance, Control, and Dynamics*, Vol. 17, No. 5, 1994, pp. 942–949.

²³Dorling, C. M., and Zinober, A. S. I., "Robust Hyperplane Design in Multivariable Variable Structure Control Systems," *International Journal of Control*, Vol. 48, No. 5, 1988, pp. 2043–2054.

²⁴Dorling, C. M., and Zinober, A. S. I., "Two Approaches to Hyperplane Design in Multivariable Variable Structure Control Systems," *International Journal of Control*, Vol. 44, No. 1, 1986, pp. 65–82.

²⁵El-Khazali, R., and DeCarlo, R., "Output Feedback Variable Structure Control Design," *Automatica*, Vol. 31, No. 6, 1995, pp. 805–816.

²⁶Kwan, C. M., "Sliding Control Using Output Feedback," *Journal of Guidance, Control, and Dynamics*, Vol. 19, No. 3, 1996, pp. 731–733.

²⁷Yallapragada, S. V., Heck, B. S., and Finney, J. D., "Reaching Conditions for Variable Structure Control with Output Feedback," *Journal of Guidance, Control, and Dynamics*, Vol. 19, No. 4, 1996, pp. 848–853.

²⁸Stevens, B. L., and Lewis, F. L., *Aircraft Control and Simulation*, Wiley, New York, 1992.

²⁹Keating, M. S., "Design of a Flight Controller for an Unmanned Research Vehicle with Control Surface Failures Using QFT," M.S. Thesis, Air Force Inst. of Technology, Wright-Patterson AFB, OH, Dec. 1993.

³⁰Keating, M. S., Pachter, M., and Houpsis, C. H., "Fault Tolerant Flight Control System: QFT Design," *International Journal of Robust and Nonlinear Control*, Vol. 7, 1997, pp. 551–559.